Applied Surface Science 410 (2017) 267–277

Contents lists available at ScienceDirect

Applied Surface Science

journal homepage: www.elsevier.com/locate/apsusc

Full Length Article

Dodecylamine functionalization of carbon nanotubes to improve dispersion, thermal and mechanical properties of polyethylene based nanocomposites

F.V. Ferreira[a,b,*], W. Franceschi[a], B.R.C. Menezes[a], F.S. Brito[a], K. Lozano[b], A.R. Coutinho[c], L.S. Cividanes[a], G.P. Thim[a]

[a] Department of Aeronautical and Mechanical Engineering, Technological Institute of Aeronautics (ITA), São José dos Campos, SP, Brazil
[b] University of Texas, Rio Grande Valley (UTRGV), Edinburg, TX, United States
[c] Laboratory of Carbon Materials, Methodist University of Piracicaba (UNIMEP), Santa Bárbara d'Oeste, SP, Brazil

ARTICLE INFO

Article history:
Received 1 February 2017
Received in revised form 8 March 2017
Accepted 9 March 2017
Available online 11 March 2017

Keywords:
Carbon nanotubes
Polymer-matrix composites (PMCs)
Mechanical testing
Thermal analysis

ABSTRACT

This study presents the effect of dodecylamine (DDA) functionalization of carbon nanotubes (CNTs) on the thermo-physical and mechanical properties of high-density polyethylene (HDPE) based composites. Here, we showed that the functionalization with DDA improved the dispersion of the CNTs as well as the interfacial adhesion with the HDPE matrix *via* non-covalent interactions. The better dispersion and interaction of CNT in the HDPE matrix as a function of the surface chemistry was correlated with the improved thermo-physical and mechanical properties.

1. Introduction

Over the past few years, the aerospace, aeronautical and automotive industries have played a key role in the active development of high-performance, low-weight and cost-effective composites [1,2]. In this context, research related to the development of materials, particularly nano-reinforced polymer composites (NRPCs), has increased significantly [3–10]. A large market opportunity emerged in the late 1990s with the introduction of NRPCs. The NRPC market is expected to grow to an estimated US$ 15 billion by 2020 [11,12]. Among the several nano-reinforcements used in NRPCs, carbon nanotubes (CNTs) play a key role.

CNTs are made exclusively of carbon atoms arranged in condensed aromatic rings with dimensions of several microns in length and few nanometers in diameter [13]. Their structure was initially described by Iijima in 1991 [14] and since then CNTs are one of the most studied materials due to their promising mechanical, electrical and thermal properties [15]. CNTs have high aspect ratios (100–1000 and higher), an estimated Young modulus of 1 TPa (the modulus of steel is approximately 0.2 TPa), 300 GPa in tensile strength (0.25 GPa for steel), and thermal conductivity values of up to 3000 $Wm^{-1} K^{-1}$ (about seven times larger than that of copper 385 $Wm^{-1} K^{-1}$) [15–19]. Therefore, CNTs have been considered one of the most attractive reinforcements for polymer, ceramic and metal matrix composites [20–24].

Composites based on polyolefin matrices have been extensively studied due to the high demand of chemically inert materials [25,26]. These composites are fabricated by three main methods: (i) *in-situ* polymerization, (ii) solution based blending and (iii) melt mixing [27,28]. Melt mixing incorporates high shear forces to promote dispersion and distribution of the nanoreinforcements [27]. However, the high viscosity and the nonpolar chemical structure of thermoplastic matrices, such as polyethylene matrices, have decreased the CNTs degree of dispersion and subsequently the interfacial interaction between CNTs and polymer matrices [15,27,29,30]. Two competitive forces contribute to the interaction and dispersion of CNTs in polymer matrices: the van der Waals forces among CNT units and the CNT chemical interactions with polymer matrices [17,31]. These forces and the high viscosity of the polymeric matrices lead to the formation of CNT aggregates, resulting in poor CNT dispersion. Surface functionalization of CNTs has proven to be an effective route to improve dispersion and chemical interaction with the matrix, consequently improving the

* Corresponding author at: Instituto Tecnológico de Aeronáutica, Praça Marechal Eduardo Gomes, 50, Vila das Acácias CEP 12228-900, São José dos Campos, SP, Brazil.
E-mail address: filipevargasf@gmail.com (F.V. Ferreira).

http://dx.doi.org/10.1016/j.apsusc.2017.03.098
0169-4332/

interfacial adhesion and thermo-physical, mechanical and electrical properties [32–34]. In this context, the functionalization with dodecylamine (DDA) promotes the formation of alkyl group (nonpolar molecule) on the surface of CNTs. Addition of this nonpolar molecule on the CNT walls could prevent agglomeration due to steric factors while effectively promoting interactions between the nanotubes and the nonpolar polymeric matrix.

There are several reports in the literature that have proved the positive effects of functionalization with DDA on the dispersion of nanomaterials in nonpolar solvents. Sobkowicz et al. [35] studied the solubility of carbon nanospheres (CNS) functionalized by DDA (CNS-DDA) in different solvents (water, chloroform and toluene). The results demonstrated that the CNS do not disperse in nonpolar solvents prior to DDA functionalization, while the DDA functionalized CNSs are effectively dispersed. The authors concluded that the dispersion of carbon nanospheres can be tailored according to the choice of functional groups attached to their surface. Ferreira et al. [36] studied the dispersion of DDA functionalized CNTs in different solvents (acetone, ethanol, xylene and water). The CNTs were treated with a mixture of concentrated H_2SO_4/HNO_3 and subsequently functionalized with dodecylamine. The results demonstrated that the CNTs subjected to the oxidation with the mixture of the acids forms aggregates in xylene (nonpolar solvent), resulting in a poor dispersion. On the other hand, the DDA functionalized CNTs are homogeneously dispersed in xylene. The authors attributed this phenomenon to the nonpolar character of the CNTs functionalized by dodecylamine, that is, the nonpolar chain of DDA attached to the surface of the nanotubes increases the nonpolar character of the CNTs and consequently improves the nanotube dispersion in the nonpolar solvent. Other authors found improvement in the mechanical properties due to the intensified interaction of the functional group attached to the surface of nanofillers and the polymer structure. Morelli et al. [37] prepared poly(butyleneadipate-*co*-terephthalate)–PBAT composites containing modified cellulose nanocrystals by 4-phenylbutyl isocyanate. They observed an increase in the elastic modulus and the tensile strength of the nanocomposites due the π-π interactions between the phenyl rings grafted onto the nanocrystals molecules and the aromatic rings of the polymeric chain.

DDA functionalized carbon nanotubes are expected to also improve its dispersion within nonpolar polymeric matrices, such as high density polyethylene (HDPE). Furthermore, since the repeating unit of HDPE is formed by an aliphatic chain, the nonpolar long chain attached to the functionalized CNT should improve wetting of the CNTs by the HDPE while providing superior interfacial compatibility given the numerous non-covalent interaction sites. The enhanced interfacial interactions often lead to an efficient load transfer and consequently an improvement in the ultimate thermo-physical and mechanical properties of the nanocomposite. These reasons prompted the study of DDA functionalized CNTs as reinforcements for HDPE based composites. To the best of our knowledge, the effects of CNT functionalization by dodecylamine on the dispersion and interfacial interaction of nanotubes into HDPE have not yet been reported.

In this study we prepared dodecylamine-functionalized carbon nanotube reinforced high density polyethylene composites by a melt mixing procedure. For comparison, nanocomposites with CNTs oxidized with a mixture of concentrated acids and unmodified CNTs were also prepared. Our results demonstrated that the nonpolar functional group attached to the functionalized CNT plays a significant role in dispersion of CNTs in nonpolar polymer matrices and it is able to promote non-covalent interactions with HDPE, thereby improving thermo-physical and mechanical properties of nanocomposites.

2. Experimental

2.1. Materials

High density polyethylene (HDPE) with a density of 0.956 g/cm^3 and melt flow rate of 50 g/10 min was purchased from Braskem. Multi-walled carbon nanotube (CNT) samples were produced by chemical vapor deposition method (pyrolysis of camphor mixed with 16 wt% of ferrocene), as previously described elsewhere [50].

2.2. CNT surface modification

2.2.1. Functionalization with carboxylic groups

Pristine carbon nanotube (CNT-H) was treated with a 3:1 mixture of concentrated sulfuric acid (H_2SO_4, Merck, 98%, 90 mL) and nitric acid (HNO_3, Vetec, 70%, 30 mL), for 6 h at room temperature in a 225 W ultrasonic bath. The modified CNT was subsequently vacuum filtered by using a cellulose nitrate filter membrane (0.45 μm pore size). Then, CNTs were washed with deionized water until the filtered water reached a neutral pH. Finally, the CNTs were dried at 40 °C for 16 h in a vacuum oven. This sample was labeled as CNT-Ac.

2.2.2. Functionalization with alkyl group (DDA)

A mixture of CNT-Ac (0.2 g) and dodecylamine (DDA, $C_{12}H_{27}N$, Sigma, 98%, 150 mL) was prepared by magnetically stirring the components for four days at 100 °C. The sample was then filtrated under vacuum using a polytetrafluorethylene (0.45 μm pore size) filter. The CNTs were then washed with ethanol (Neon, 95%) to remove any residual DDA. Finally, the CNTs were dried in a vacuum oven at 40 °C for 16 h. This sample was labeled CNT-DDA. Fig. 1 shows a schematic representation of the process.

2.3. Methods

Carbon nanotubes were first dispersed in acetone in an ultrasonic bath for 30 min. Then, the HDPE pellets were added to the previous solution and mixed under magnetic stirring for 30 min. After that, the mixture was dried at 80 °C for 4 days to remove the acetone. Dry, solid HDPE pellets coated with CNTs were obtained. These pellets (covered with 0.8 wt.% CNTs) were melted in a heating mantle (Arsec AQ22B) at 205 °C. The melt was mechanically stirred (IKA RW 20) at 200 rpm. Subsequently, the highly viscous melt was poured into an aluminum mold and placed in a vacuum oven at 205 °C at an absolute pressure of 0.2 bar for 1 h to remove left over air bubbles, followed by casting under compression (5 Kgf). Finally, the NRPC was left to cool at ambient temperature.

2.4. Characterization

Fourier transform infrared (FT-IR) analysis was conducted in a Spectrum One FT-IR spectrometer (PerkinElmer) (resolution 4 cm^{-1}, 40 scans) utilizing the KBr pellet technique (0.2:400 mg), in the 4000–400 cm^{-1} range. X-ray photoelectron spectroscopy (XPS) analysis of the carbon nanotube samples was performed on a commercial spectrometer (UNI-SPECS UHV), with Mg Kα line ($h\nu$ = 1253.6 eV) and a pass energy set at 10 eV. The composition of the surface layer was determined from the ratio of the relative peak areas corrected by the Scofield sensitivity factors for the corresponding elements. The width at half maximum (FWHM) varied between 1.2 and 2.1 eV and the accuracy of the peak positions was ±0.1. The microstructure of the carbon nanotubes was characterized using a transmission electron microscope (TEM), FEI-TECNAI G2 with an accelerating voltage of 200 kV.

The dispersion behavior of carbon nanotubes in solvents was analyzed based on visual observations. CNTs were dispersed in water and xylene at concentrations of 0.1 mg.mL^{-1}. The solution

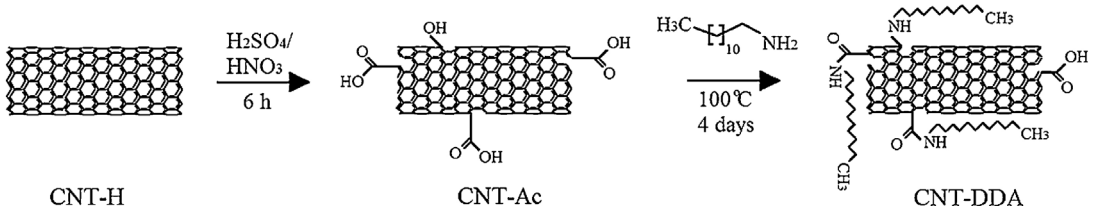

Fig. 1. Schematic representation of the functionalization process.

was sonicated (Branson 2210,125 W) for 30 min and the images were taken 24 h after sonication. The dispersion states were classified in two groups: dispersed and sedimented. Samples were labeled as "dispersed state" if the nanotube/solvent mixture formed a dark solution with no visual aggregation and precipitation after 24 h, while the "sedimented state" was related to samples where the nanotubes precipitated after 24 h.

The morphology of CNT/HDPE composites was examined using a field emission gun-scanning electron microscope (Philips FEG-SEM). Cross sections of the samples were prepared by fracturing the samples under cryogenic conditions. Dynamic mechanical analysis (DMA) measurements were carried out by using a DMA Q 800 (TA Instrumental Company); samples were analyzed under a constant frequency of 1 Hz from room temperature to 220 °C at a heating rate of 3 °C/min. The sample dimensions were $(60 \times 12 \times 3)\,mm^3$. At least three samples were analyzed to ensure sample reproducibility. Calorimetry studies were performed using a Pyris DSC (Perkin-Elmer) Model with aluminum pans. All samples (around 8 mg) were heated from room temperature to 220 °C with a heating rate of 5 °C/min and kept at 220 °C for 2 min. Then, samples were cooled to 30 °C with cooling rates of 10 °C/min under nitrogen atmosphere. Thermogravimetric analysis (TGA) was carried out using a TGA 7HT Perkin Elmer, samples were analyzed from 25 to 800 °C, at 10 °C/min in air. Hardness testing was conducted using loads of 0.5 N and applied for 30 s. Studies were conducted in a Diamond Vickers indenter Tester FM-700. Thirty two well-separated indents were made on each surface (keeping the appropriate distance from sample edges and between indentation marks) and random regions were selected to verify data consistency. The hardness value HV (in GPa) was calculated from the indentation load and the diagonal of the Vickers imprint. The HV data set was statistically analyzed (confidence interval of 95%) using the R program (statistical computational and graphical environment).

3. Results and discussion

3.1. Fourier Transform Infrared (FT-IR) spectroscopy

FT-IR spectroscopy (Fig. 2) was used to qualitatively evaluate the changes produced by functional groups on the surface of CNTs. All spectra showed bands at approximately 3445 and 1630 cm^{-1}, which correspond to the O—H and C=C stretching vibrations, respectively [32,38]. Additionally, all FT-IR spectra showed bands at 2920 and 2850 cm^{-1} corresponding to asymmetric (νa CH_2) and symmetric (νs CH_2) stretching vibrations of the methylene group, which are usually assigned to defects in rings of CNTs [38–40]. FT-IR spectrum of CNT-Ac showed the appearance of a band at 1726 cm^{-1}, which is associated with the carbonyl stretch of the carboxylic acid group [33,38,41]. Further confirmation of the oxidation process comes from the intense double band at 2920 and 2850 cm^{-1}. According to a previous study [42], the presence of carboxylated CNT increases the intensity of this double band. This increase is due to the presence of hydroxyl and carboxyl groups covalently attached to the CNT during the surface modification with H_2SO_4/HNO_3. This covalent linkage induces

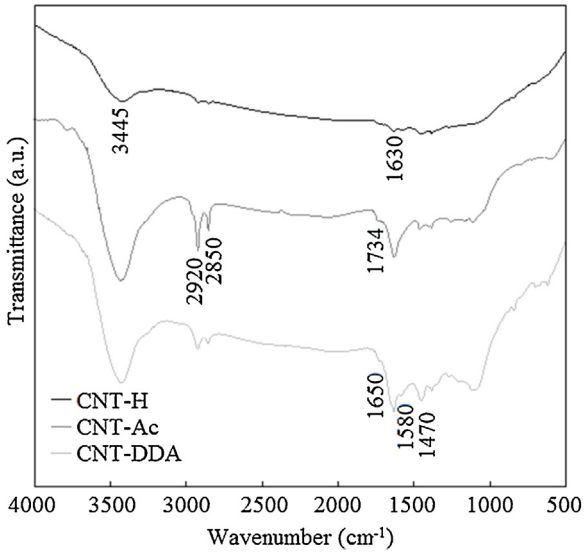

Fig. 2. FT-IR spectra of CNT-H, CNT-Ac and CNT-DDA.

Table 1
Surface composition of CNTs at different stages determined by XPS deconvolution.

Chemical bond	Peak (eV)	CNT-H	CNT-Ac	CNT-DDA
C—C sp^2	284.4	70.1	63.7	36.5
C—C sp^3	285.2	14.5	14.2	42.1
C—O, C=O, O—C=O	286.3–289.2	11.4	18.7	13.6
C—N	285.8	–	–	7.3
π–π^*	291.0	4.0	3.4	0.5

defects in the nanotube structure, changing sp^2 hybridized C—C to sp^3 hybridized C—C bonds [43]. After functionalization with alkyl groups, bands at approximately 1580 and 1470 cm^{-1} were observed in the spectrum, which may be assigned to N—H and C—N stretching, respectively [38]. Furthermore, the band at 1726 cm^{-1} almost disappeared and a new band at 1650 cm^{-1} appeared, suggesting the formation of amide functional groups (—(C=O)—NH—) on CNT-DDA [33,38]. As reported by Rahimpour et al. [42] and Ma et al. [44], the coupling reaction of the amine functional groups occurs between the DDA and the carboxylic groups of the carboxylated CNTs, forming amide and H_2O. Thus, the FT-IR spectrum of CNT-DDA confirms that the surface of CNT-Ac was successfully modified by the amine functional groups.

3.2. X-ray photoelectron spectroscopy (XPS)

XPS analysis was performed in order to quantitatively investigate the surface of the CNTs. The survey spectra in Fig. 3a confirm the presence of C1s and O1s peaks in all samples, while N1s exists only in the dodecylamine-modified CNTs sample. The C1s XPS peak of each sample was deconvoluted to better reveal the functionalization process. The deconvolution results are shown in Table 1. C—C species (sp^2 hybridized carbon atoms) decreased after each step of

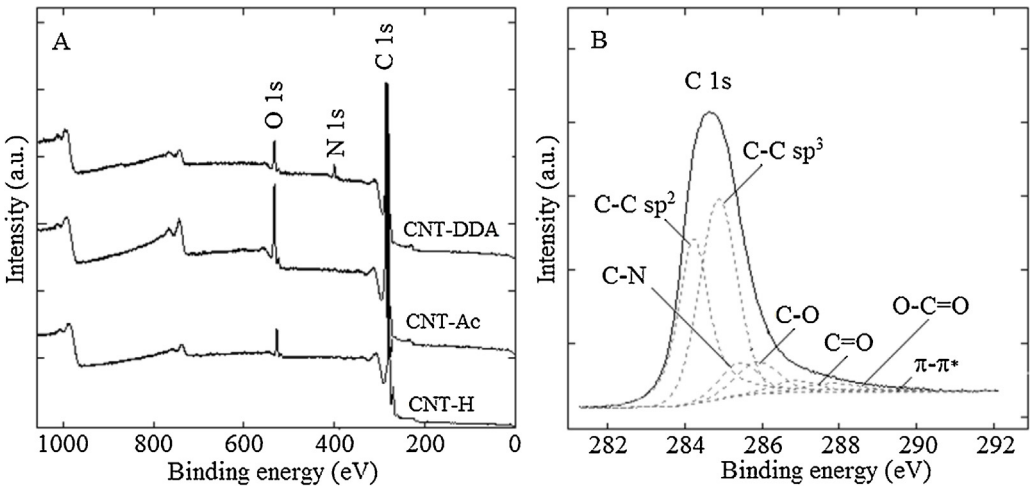

Fig. 3. (a) XPS survey spectra of CNTs and (b) deconvoluted of C1s XPS spectrum.

the surface treatment, which is related to the presence of strong oxidants used in the surface modifications. As discussed above, the covalent functionalization attained during the H_2SO_4/HNO_3 treatment occurs by a change in the carbon hybridization with simultaneous loss of the local conjugation. This observation has also been concluded in other reports where other reagents have been reported to damage the CNT walls breaking the —C=C— double bonds and consequently decreasing the sp^2 C—C contents. Soares et al. [41] investigated carbon black functionalized by alkyl group using dodecylamine. The XPS results of this work showed that the peak at 284.1 eV (sp^2 C—C) decreased in intensity from 76.02 to 48.45% after surface modification with DDA.

The oxygen content increased from 11.4 to 18.7%, when CNT-Ac was compared to the CNT-H samples. This indicates that oxygen-containing functional groups were successfully introduced onto the surface of the CNTs after oxidation with H_2SO_4/HNO_3. Additionally, the sp^3 C—H species slightly decreased (from 14.5 to 14.2%), suggesting that the acid treatment removes some amorphous carbon from the nanotube walls. Early studies [45–47] have reported that two competitive processes occur during the surface modification with strong oxidizers: (i) the oxidation induces some defects due to the anchorage of functional groups on the CNT walls and (ii) the treatment removes the defects (amorphous carbon and metal catalysts) of the CNTs. Thus, the slight decrease of sp^3 C—H here observed derives from the "ii" processes (removal of amorphous carbon of the nanotube walls). On the other hand, the oxygen content decreased after the surface modification by dodecylamine. This behavior is related to the H_2O formation due to the coupling reaction between DDA and carboxylic groups on the surface of CNT, as mentioned above in the FT-IR analysis. Simultaneously, the sp^3 C—H species increased due to the long carbon chain contained in dodecylamine molecules attached to the surface of the nanotube after DDA functionalization [41]. Moreover, the XPS spectrum of the CNT-DDA showed a new peak corresponding to the N1s (around 400.0 eV), which is due to the nitrogenated functional group incorporated on the CNT-DDA surface [31,44]. Similar behavior was also observed by other researchers [48] when working with alkane-modified CNT. They reported that the oxygen content decreased about 1.9% after dodecylamine functionalization, while the N content of functionalized CNT sample increased 0.9%. The authors attributed these changes to the coupling reaction between the amine and carboxylic groups on the surface of CNTs. Therefore, the XPS results confirm the covalent modification of the CNT surface, which supported the results obtained by FT-IR analysis.

3.3. Transmission electron microscope (TEM)

Fig. 4 shows TEM images of CNT-H, CNT-Ac and CNT-DDA. Fig. 4a shows the presence of black spots within the structure of the CNT-H sample, these are attributed to metal impurities (CNTs were produced with camphor/ferrocene). The micrograph of the unmodified CNTs shows poor dispersion, carbon nanotubes have large surface area, which enhances its tendency to aggregate [38]. After the functionalization process (Fig. 4c and e), the presence of black spots decreases. Moreover, the introduction of functional groups (carboxyl and alkane groups) on the surface of the CNTs creates electrostatic charges which decrease the strong self-interaction of carbon nanotubes, less entanglement is observed and results in an enhanced dispersion and distribution of the nanotubes [31,45,46].

The structural integrity of the nanotubes was also analyzed by TEM. CNT-H (Fig. 4b) showed relatively smooth and homogeneous sidewalls, while samples functionalized with carboxylic groups (Fig. 4d) showed thicker sidewalls. The alkane-modified CNT (Fig. 4f) also exhibited a rougher surface as well as an increase in wall defects (dark area in the walls) compared to the CNT-Ac samples. Moreover, Fig. 4f shows that the CNT-DDA sample displays an additional outer layer which lacks the characteristic lines of concentric CNTs. This outer layer is related to the dodecylamine molecules attached to the surface of the nanotube. The structural damage observed on the surface of the carbon nanotubes after each step of the surface treatment is related to the significant effect of the strong oxidizing agents on the graphitic surface of the material. This assumption was confirmed by the decrease of sp^2-hybridized carbon atoms observed in the XPS results. Changes on the structural integrity of the nanotubes after surface modification have been observed by a number of groups [31,46]. Yang et al. [31] have prepared CNT functionalized with H_2SO_4/HNO_3, followed by triethylenetetramine (TETA) reaction with the carboxylic acid groups. Their TEM observations showed that the surface of the carbon nanotubes becomes rough after surface modification, which is attributed to a TETA thin layer formed on the nanotube wall. In additional, the authors reported that this thin layer plays an important role in order to prevent the agglomeration of the CNT and may serve to establish stronger interactions between the CNTs and the polymeric matrix.

3.4. Dispersion analysis

Fig 5 shows the dispersion states of unmodified and modified CNTs in water and xylene. Unmodified CNTs were completely non-dispersible in both solvents, and the dispersion state was eval-

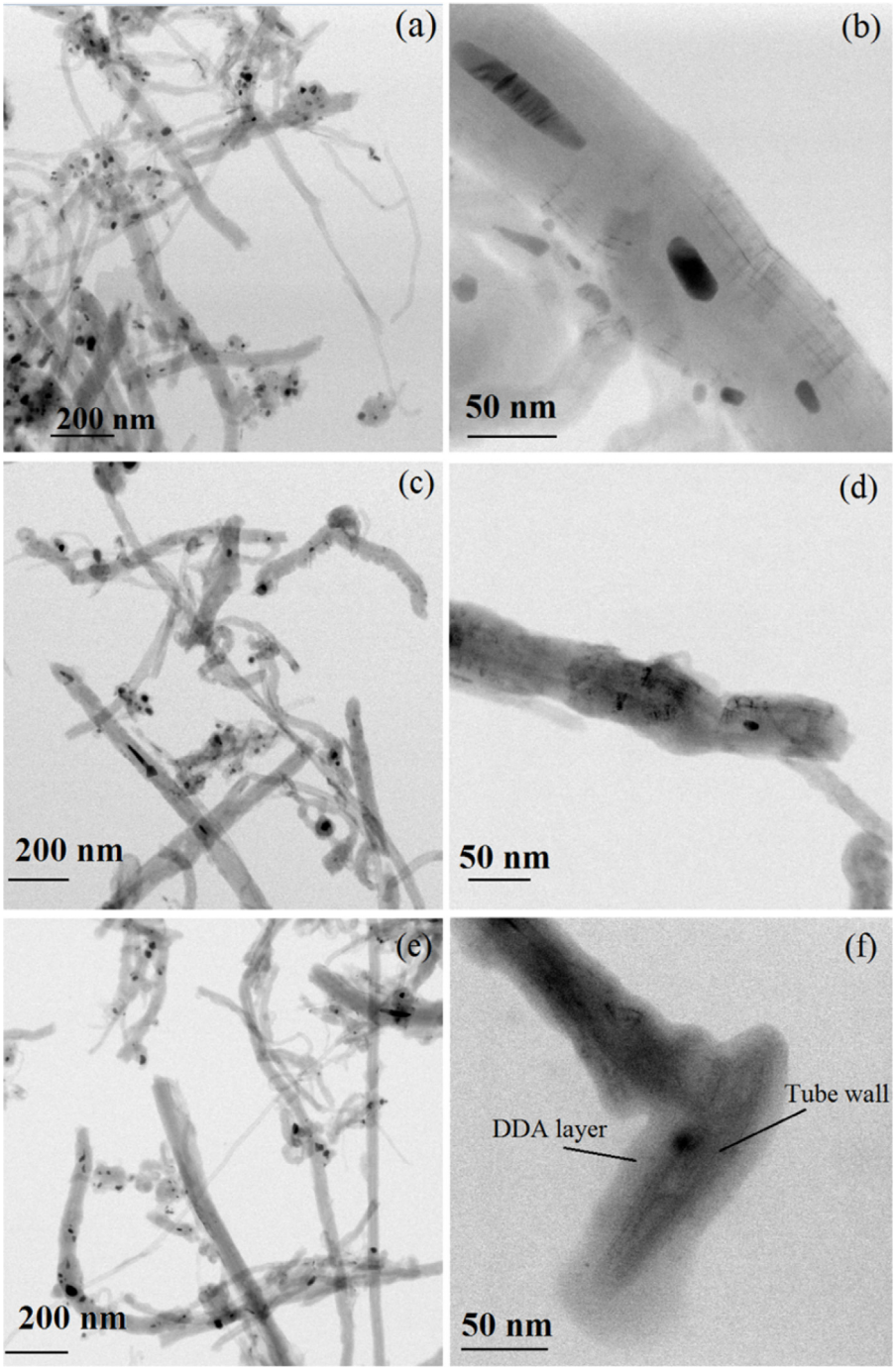

Fig. 4. Transmission electron micrographs of (a and b) CNT-H, (c and d) CNT-Ac and (e and f) CNT-DDA.

uated as sedimented. This behavior is related to self-interactions of carbon nanotubes due to van der Waals attraction [38]. On the other hand, the dispersibility of carbon nanotubes in water was remarkably changed after the oxidation with H_2SO_4/HNO_3 and the dispersion state was classified as dispersed. The reasons for these occurrences are the polar groups (carboxylic groups) covalently attached on the CNT walls during surface modification with acid. These groups not only decrease the self-interaction of carbon nanotube, but they also increase the polar character of the nanotubes, improving interaction between CNT-Ac and polar solvents by chemical similarity [36]. After the functionalization with dodecylamine, the dispersion state of CNT-DDA in water was classified as sedimented, while the dispersion in xylene was classified as dispersed. This behavior is related to an enhanced nonpolar character of the CNTs due to the nonpolar chain of DDA attached to the nanotube surface. Some studies have shown that the dispersibility of carbon nanomaterials can be tailored according to the groups grafted onto their surface. Vukovicí et al. [38] studied the dispersibility of CNTs in water. In this work, the CNTs were oxidized by a mixture of concentrated H_2SO_4 and HNO_3, and then functionalized by four different amines: diethylenetriamine (DETA); triethylenetetramine (TETA); 1,6-hexanediamine (HDA) and 1,4-phenylenediamine (PDA). The study revealed that oxidation introduces polar groups on the surface of CNTs, creating the electrostatic stability required for a stable dispersion in water. However, the same dispersion behavior was not observed for the

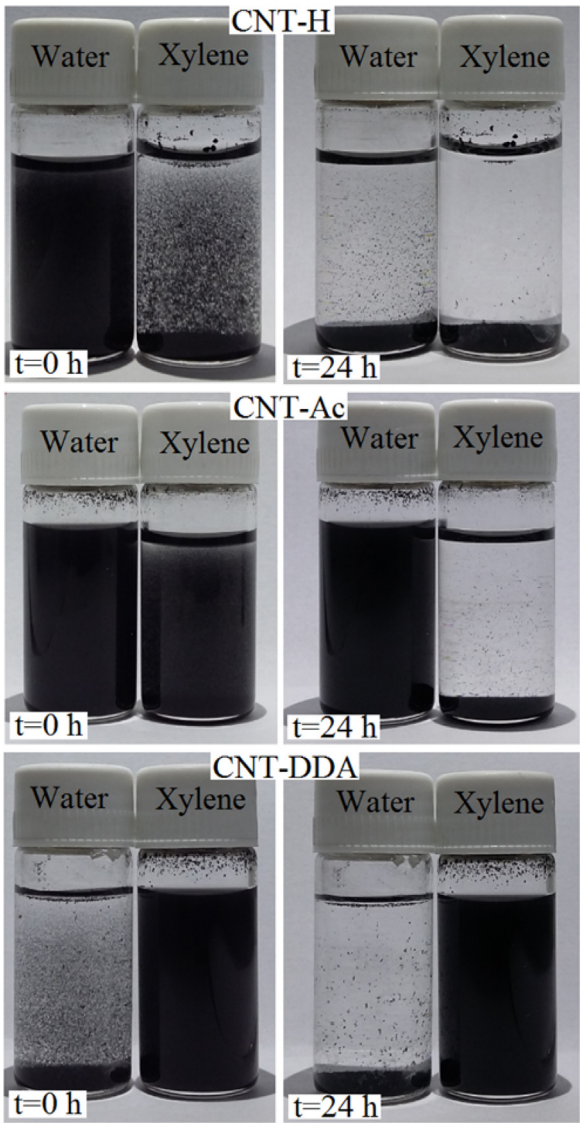

Fig. 5. Dispersion states of unmodified and modified CNTs in water and xylene at a concentration of 1 mg mL^{-1}.

amino-functionalized CNTs. The authors reported that the dispersion of functionalized nanotubes is dependent on the structure of the amine presented onto the CNT surface, as well as the solvent used. In another study [35], carbon nanospheres (CNS) were functionalized with a 12-chain alkylamine (dodecylamine). The results demonstrated that the CNSs were completely undispersable in nonpolar solvents such as toluene. However, after covalent surface grafting of dodecylamine, the toluene solubility of alkane-modified CNS was remarkably improved. Based on this prior knowledge, a stronger interaction among the dodecylamine-modified CNTs and nonpolar polymeric matrices is expected. It may open the path to simplify CNT manipulation and processing of composites with nonpolar polymeric matrix.

3.5. Scanning electron microscopy (*SEM*)

Dispersion of CNTs in the polyethylene matrix was analyzed by scanning electron microscopy of cryogenically fractured cross sections. Fig. 6 shows SEM micrographs of CNT reinforced HDPE composites. Carbon nanotube can be clearly identified in the area marked with a red square in the SEM micrographs of the unmodified CNT/polyethylene composite (Fig. 6a) and the formation of agglomerates is observed. These agglomerates weaken the composite, decreasing their mechanical properties. Acid oxidation promoted a better dispersion, as can be observed in Fig. 6b. However, the interface between CNT-Ac and polyethylene is weak (poor wetting), as many CNTs pulled out of the matrix. The poor wetting occurs due to the difference in polarity between polar groups on the CNT-Ac surface interacting with the nonpolar HDPE matrix. CNT-DDA/HDPE composites (Fig. 6c) shows improved separation of nanotube bundles and improved interfacial interaction among the carbon nanotube with the polymeric matrix, CNT-DDA are breaking rather than being pulled-out. This behavior relates to the improved compatibility between the CNT-DDA and the nonpolar polymeric matrix. The dispersion and interaction of nanofillers in polymeric matrices as a function of functional group attached to nanofillers surface and the polymer structure have also been previously demonstrated. Pang et al. [49] prepared functionalized graphene oxide with octadecylamine (ODA-GO) and fabricated ODA-GO/CNT/HDPE/UHMWPE composites by solution mixing and high-speed mechanical mixing. The results showed that the presence of the long octadecyl chains promotes homogeneous dispersion of the ODA-GO in the polymeric matrix. Furthermore, octadecyl chains intensify the adhesive interaction between the ODA-GO and the polyethylene chains, contributing to the reinforcement effect. Morelli et al. [37] prepared poly(butyleneadipate-*co*-terephthalate)–PBAT composites containing cellulose nanocrystals (CNC) through solvent casting. The surface of the CNCs was modified by 4-phenylbutyl isocyanate to improve dispersion and compatibility with the polymer matrix. The authors attributed the improved mechanical properties of the composite with modified cellulose nanocrystals to the π-π interactions between the phenyl rings grafted onto the CNC molecules and the aromatic rings of the polymeric chain. Furthermore, other features can be listed as playing an important role to improve the interfacial interaction, such as the surface structure of carbon nanotubes. Barber et al. [51] realized some pullout experiments and concluded that the damaged CNT can interact with the surrounding polymer matrix through defects in the nanotube structure, since the unmodified nanotubes are atomically smooth.

We can therefore infer that the good dispersion and superior interfacial compatibility between the CNT-DDA and the nonpolar polymeric matrix may be related to non-covalent bonding between the nonpolar long chain attached to the CNT surface functionalized by DDA and the aliphatic chain of HDPE. The rougher surface of CNT-DDA observed in TEM micrographs (Fig. 4f) may have also contributed to strengthen the interface. This combination resulted in an enhanced load transfer effect to the nanotube network.

Table 2
Variation of E' and E" of HDPE and CNT/HDPE composites.

Sample	E′ at 27 °C (MPa)	E" at 27 °C (MPa)	tan δ
HDPE	1278 ± 4.8	115 ± 4.3	0.090 ± 0.0002
CNT-H/HDPE	1319 ± 1.0	124 ± 1.4	0.094 ± 0.0001
CNT-Ac/HDPE	1398 ± 2.3	131 ± 1.6	0.094 ± 0.0004
CNT-DDA/HDPE	1465 ± 2.3	137 ± 0.6	0.094 ± 0.0001

3.6. Dynamic mechanical analysis (DMA)

The viscoelastic properties of the neat polyethylene and composites filled with different carbon nanotubes were characterized by dynamic mechanical analysis. The variation of the dynamic storage modulus (E′), loss modulus (E″) and the damping factor (tan δ) of the samples is presented in Fig. 7. The values of E′ and E″ at 27 °C are summarized in Table 2. The increase of the storage modulus of CNT-H/HDPE composites of about 3% compared with pure HDPE, indicated an effective reinforcement of the carbon nanotubes. Fur-

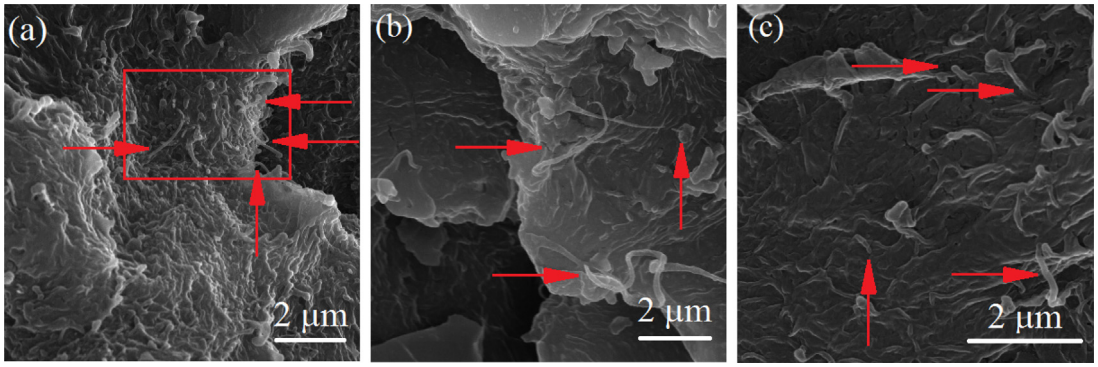

Fig. 6. SEM microphotographs of the samples (a) CNT-H/HDPE, (b) CNT-Ac/HDPE and (c) CNT-DDA/HDPE.

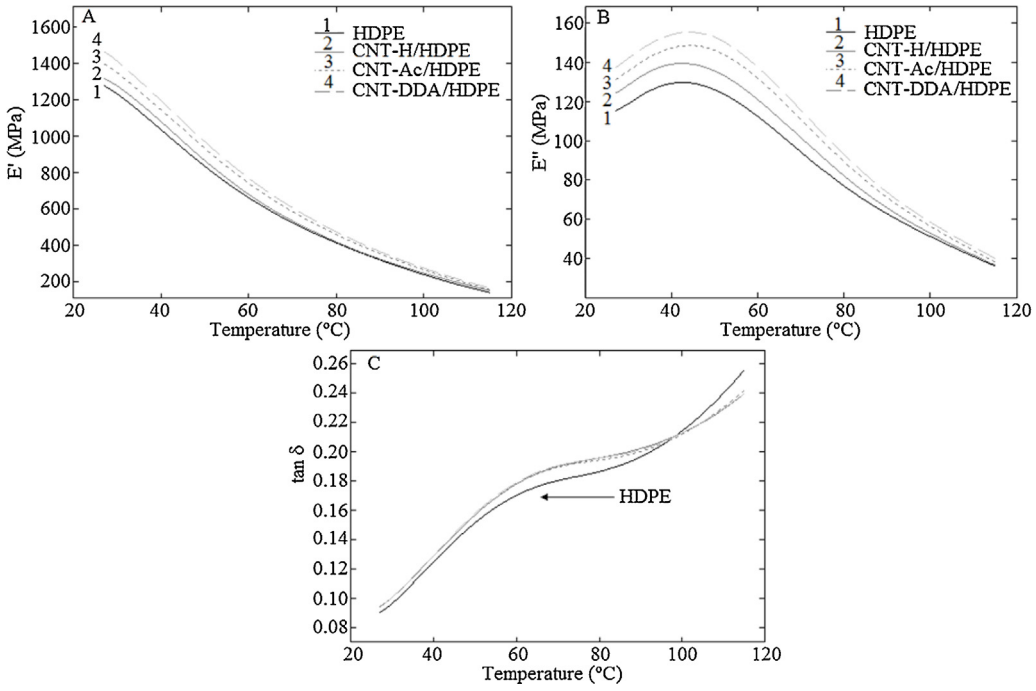

Fig. 7. (a) Storage modulus, (b) loss modulus and (b) tan δ of HDPE and CNT/HDPE composites.

thermore, E′ of the composites gradually increase after each step of the surface modification, especially at lower temperatures. At 27 °C, the storage modulus of CNT-Ac/HDPE increased about 6% from values observed for the CNT-H/HDPE, while CNT-DDA reinforced polyethylene composites show the largest improvement, about 4.8% when compared to the CNT-Ac/HDPE sample, and about 14.6% when compared to the HDPE sample. Similar behavior was also observed by other researchers when analyzing the effects of the incorporation of carbon nanotube on the mechanical behavior of polypropylene [52]. They prepared single-walled carbon nanotubes (SWNTs)/polypropylene (PP) nanocomposites through shear mixing and found that the modulus of the composites with 0.75 wt% SWNTs increased from 855 to 1187 MPa when compared to pure polymer.

Fig. 7b shows that the loss modulus behavior is similar to that one observed for the storage modulus: CNT-DDA > CNT-Ac > CNT-H. This behavior is also directly related to the improved carbon nanotube dispersion throughout the HDPE matrix. The addition of carbon nanotube to the HDPE matrix leads to a mesophase formation between the CNT and matrix [53]. This mesophase contributes to dissipate energy from external stresses by frictions between particle–particle and particle-polymer interaction. The improved dispersion of CNTs and enhanced interfacial interactions with the polyethylene contribute to the dissipation of energy throughout the matrix, giving rise to both dynamic modulus [54,55].

The damping factor (tanδ) is a measure of the contributions of the viscous and elastic components of a viscoelastic material and can be determined by the ratio of loss modulus to storage modulus (E″/E′) [54,55]. The results of tanδ are plotted in Fig. 7c, which shows an increase in the damping peak for the composites when compared to the neat HDPE. Assuming that the damping peak is directly related to the degree of crystallinity of the polyethylene [56,57], it can be observed that the addition of CNT in HDPE may have influenced the polymer crystallinity, as discussed below.

3.7. *Differential scanning calorimetry (DSC)*

Thermal analysis of the composites was performed in order to assess the influence of carbon nanotube on the crystallinity of the polyethylene matrix. The DSC curves are presented in Fig. 8. From the DSC curves, the enthalpy of fusion (ΔH_m), the crystallization temperature (T_c) and crystallization enthalpy (ΔH_c) were obtained

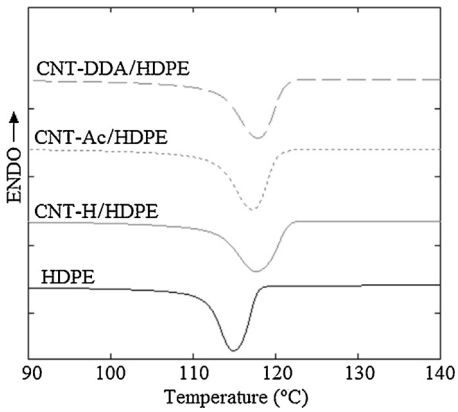

Fig. 8. DSC thermograms of CNT/HDPE composites with cooling rates of 10 °C/min under nitrogen atmosphere.

Table 3
Values of ΔH_m, T_c, ΔH_c and X_c of HDPE and CNT/HDPE nanocomposites.

Sample	ΔH_m (J/g)	T_c (°C)	ΔH_c (J/g)	X_c (%)
HDPE	179.6 ± 2.3	115.1 ± 0.2	150.4 ± 2.2	61.8
CNT-H/HDPE	192.1 ± 3.9	118.0 ± 0.2	159.2 ± 3.3	66.1
CNT-Ac/HDPE	188.8 ± 1.1	117.1 ± 0.1	159.1 ± 0.1	65.0
CNT-DDA/HDPE	191.6 ± 1.3	118.0 ± 0.1	159.7 ± 1.4	66.0

and reported in Table 3. The crystallinity (X_c) is calculated according to the following equation:

$$X_c = \frac{\Delta H_m}{293 f_c}, \quad (1)$$

where ΔH_m is the measured enthalpy of fusion (J/g), 293 J/g is the enthalpy of fusion for 100% pure crystalline HDPE [58] and fc is the weight fraction of the polymer [59].

The crystallization temperature (T_c) of the composites was shifted to a temperature slightly higher than that of pure HDPE, indicating that there are interactions between the filler and the matrix. Since the increase in T_c is directly related to an increased number of heterogeneous nuclei for crystallization [52], the results demonstrated that carbon nanotubes act as nucleating agents (nucleation sites). This nucleating activity was also reported in a previous study of CNT/HDPE composites [58] and CNT/polypropylene composites [60]. In addition, ΔH_c also increased together with X_c. This increase in crystallinity is related to the enhanced interfacial interaction among CNT and the matrix [58]. There are many studies related to the interface of polymer-CNT composites, but the morphology and properties of the polymer at the interface is not fully understood. Coleman et al. [61] and Barber et al. [62] reported that the morphology and properties of the polymer at the interface immediately surrounded by CNTs are different from those of the bulk. Assouline et al. [60] reported that the insertion of CNTs affects the overall morphology of the polypropylene. Accordingly, the polymer appears to crystallize in a fibrillar structure in the nanocomposite, while the spherical structure is observed in the pure polymer. In another work, Coleman et al. [63] were able to link the morphology and properties of the polymer to the formation of a high strength crystalline coating at the interface. Keeping the same principles in mind, the insertion of CNT should have affected the HDPE morphology at the interface, increasing the crystalline content. However, it should be pointed out that spherulitic morphology is very specific to each polymer. Thus, more work is needed to understand the mechanism that leads to such morphology and their relationship with the crystallinity of the polymer.

Table 4
TGA results of HDPE and composites CNT/HDPE under air.

Sample	T_{ONSET} (°C)	T_{MAX} (°C)
HDPE	350.1	435.1
CNT-H/HDPE	352.9	436.3
CNT-Ac/HDPE	359.6	437.5
CNT-DDA/HDPE	363.2	439.1

Although there is much discussion regarding the nature of the polymer at the interface, it is clear that the interfacial interaction of the CNT/polymer at the interface depends on the properties of the matrix and filler, but more importantly on their interaction. Moreover, this interaction plays an important role in the mechanical reinforcement process [61]. Accordingly, as the interfacial order increases, the total binding energy of the CNT-polymer also increases, resulting in an improved interfacial stress transfer [58]. Thus, the addition of CNT, in particular alkane-modified CNT, positively affects the mechanical properties of the composites.

3.8. Thermogravimetric analysis (TGA)

The thermal stability of HDPE and the CNT/HDPE composites was analyzed under an air atmosphere using thermogravimetric analysis. The onset temperature (T_{ONSET}; temperature at which 5% weight loss occurs) and degradation temperature (T_{MAX}; peak of the derivative TGA curve) were chosen to describe the thermal stability of the samples [64]. Usually, an increase in T_{ONSET} and T_{MAX} suggests an improvement in thermal stability. The values are summarized in Table 4. T_{ONSET} and T_{MAX} increased with the addition of carbon nanotube in the polyethylene. In addition, the CNT-DDA/HDPE composite exhibited the highest value in both temperatures, suggesting a greater thermal stability of the nanocomposite. The enhanced thermal stability of the CNT-DDA/HDPE nanocomposite may be attributed to the uniform dispersion and improved interfacial interaction between the CNT-DDA and polyethylene. Shi et al. [64] reported that the difference in thermal stability between the unmodified-CNT/HDPE and modified-CNT/HDPE composite may be related to the structural difference of the CNTs and the pyrolysis mechanism of each composite. Kiula et al. [65] reported that the homogeneous dispersion of the filler can act as a barrier to the oxygen supply during thermal degradation on the surfaces of the nanocomposites, enhancing thermal stability of the nanocomposites. Other authors observed that the dispersion and interaction between the filler and the matrix are strongly associated with gas permeation properties, since the good dispersion and improved interfacial interaction promote a “tortuous path” to the molecules of the oxidizing gas that permeates through the nanocomposites materials [65–67].

3.9. Hardness test

Fig. 9 shows the results obtained from Vickers hardness testing. The measured hardness for the pure HDPE matrix was 5.1 HV and it increased to 7.5 HV with the addition of CNT-H. An increase of about 47% is obtained when compared to the HDPE samples. Hardness values for the CNT-Ac/HDPE (7.4 HV) are similar to those of CNT-H (7.5 HV) (Fig. 9b and c). As mentioned above, steric hindrance contributions resulted in enhanced dispersibility of the acid functionalized carbon nanotubes. However, the molecular interactions between CNT-Ac and nonpolar polymers are low. Consequently, the poor wetting of the filler by the matrix hinders an efficient load transfer effect given the poorly developed interface. The highest hardness value (7.7 HV) was observed for CNT-DDA based composites. An increase of about 50% is obtained when compared to the HDPE sample and an increase of about 4% when compared

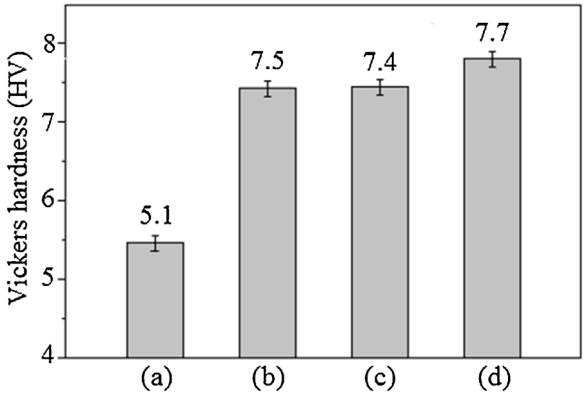

Fig. 9. Vickers hardness of the samples (a) HDPE, (b) CNT-H/HDPE, (c) CNT-Ac/HDPE and (d) CNT-DDA/HDPE.

to the CNT-Ac/HDPE sample, dodecylamine-modified CNTs show stronger interactions with the HDPE than the CNT-Ac.

Some authors working with amine-modified CNT and other polymeric matrices, especially epoxy resins, have observed higher increments in the thermo-mechanical properties of the nanocomposites [68]. The amino group attached on the modified CNT bonds covalently to epoxy resins, whereas in the case of the CNT-DDA samples, the prevalent bonding occurs by non-covalent interactions (van der Waals interactions) with HDPE. This conclusion is supported by computer simulation work [69,70], in which the interfacial strength of a CNT/polyethylene system predicted that using the covalent bonding is an order of magnitude greater (50 times) than those using the van der Waals interactions.

The obtained results allow us to conclude that the overall improvements are from a synergistic effect of the improved dispersion of CNTs-DDA in the matrix and the non-covalent interfaces obtained by van der Waals interactions among the nonpolar chain of DDA and the polyethylene matrix.

Nanocomposites based on CNT and thermoplastic matrices are lighter than their metal counterparts and offer enhanced geometric conformability when compared with CNC-based thermoset matrix [71]. They are currently of great interest for use in a wide variety of potential applications, such as materials to shield electromagnetic interference and as electronic devices, transducers and sensors (chemical and pressure) [72,73]. Despite this wide applicability, there are still many challenges and opportunities waiting to be surmounted and seized in this field. While *in situ* polymerization, high power ultrasonic mixers, and functionalization of CNTs have been a convenient route to produce CNT-based polymer nanocomposites, these techniques may be not commercially viable and environmentally friendly [27,59,74]. In additional, some of the intrinsic properties of CNTs, such as thermal conductivity and Young modulus, could be altered given the presence of the functional groups and defects created by the chemical functionalization routes [75,76]. Therefore, further understanding of the surface modification of CNT and the manufacturing of CNT-based polymer nanocomposites is needed in order to develop materials that meet durability, performance, weight, and cost required to meet commercial needs. More research in this field is thus expected.

4. Conclusions

The carbon nanotube functionalization decreases their graphitic nature. The oxidation with concentrated acids enables the dispersion of the CNTs in polar solvent, while the functionalization with DDA enables the dispersion of CNTs in nonpolar solvent. Additionally, both surface modification leads to the good dispersion of the CNTs within the HDPE matrix, whereas only the dodecylamine modification enhances the interfacial bonding between the CNTs and HDPE matrix through van der Waals interactions, thereby improving the mechanical and thermal properties of the nanocomposites. The study here presented promotes further understanding of CNT functionalization mechanisms and its effect on the overall properties of polymeric composites.

Acknowledgements

The authors acknowledge FAPESP (Grants 2013/20218-0 and 2014/17492-6) and CNPq (Grant 141197/2014-5) for financial support, and LAS/INPE and LEFE/UNESP for their collaboration. The authors also gratefully acknowledge support received by NSF PREM award under grant No. DMR-1523577:UTRGV-UMN Partnership for Fostering Innovation by Bridging Excellence in Research and Student.

References

[1] O. Gohardani, M.C. Elola, C. Elizetxea, Potential and prospective implementation of carbon nanotubes on next generation aircraft and space vehicles: a review of current and expected applications in aerospace sciences, Prog. Aerosp. Sci. 70 (2014) 42–68, http://dx.doi.org/10.1016/j.paerosci.2014.05.002.
[2] F.V. Ferreira, L.S. Cividanes, F.S. Brito, B.R.C. de Menezes, W. Franceschi, E.A.N. Simonetti, et al., Functionalization of Carbon Nanotube and Applications, 2016, pp. 31–61, http://dx.doi.org/10.1007/978-3-319-35110-0_2.
[3] T.V. Duncan, Applications of nanotechnology in food packaging and food safety: barrier materials, antimicrobials and sensors, J. Colloid Interface Sci. 363 (2011) 1–24, http://dx.doi.org/10.1016/j.jcis.2011.07.017.
[4] D.R. Paul, L.M. Robeson, Polymer nanotechnology: nanocomposites, Polymer 49 (2008) 3187–3204, http://dx.doi.org/10.1016/j.polymer.2008.04.017.
[5] J. Lu, S.X. Lim, C.H. Sow, A focused laser beam: a useful and versatile tool for 1D nanomaterials research: a review, J. Mater. Sci. Technol. 616 (2015) 616–629, http://dx.doi.org/10.1016/j.jmst.2014.12.006.
[6] A. Ameli, M. Nofar, C.B. Park, P. Pötschke, G. Rizvi, Polypropylene/carbon nanotube nano/microcellular structures with high dieletric permittivity, low dielectric loss, and low percolation threshold, Carbon 71 (2014) 206–217, http://dx.doi.org/10.1016/j.carbon.2014.01.031.
[7] S. Azoz, L.M. Gilbetson, S.M. Hashmi, P. Han, G.E. Sterbinsky, S.A. Kanaan, et al., Enhanced dispersion and electronic performance of single-walled carbon nanotube thin films without surfactants: a comprehensive study of various treatment process, Carbon 93 (2015) 1008–1020, http://dx.doi.org/10.1016/j.carbon.2015.05.087.
[8] M.A. Kabbani, C.S. Tiwary, A. Som, R. Krishnadas, P.A.S. Autreto, S. Ozden, et al., A generic approach for mechano-chemical reactions between carbonnanotubes of different functionalities, Carbon 104 (2016) 196–202, http://dx.doi.org/10.1016/j.carbon.2016.02.094.
[9] W. Tie, S.S. Bhattacharyya, Y. Zhang, Z. Zheng, T.H. Lee, S.W. Lee, et al., Field-induced stretching and dynamic reorientation of functionalized multiwalled carbon nanotube aggregates in nematic liquid crystals, Carbon 96 (2016) 548–556, http://dx.doi.org/10.1016/j.carbon.2015.09.096.
[10] D. Micheli, A. Vricella, R. Pastore, A. Delfini, A. Giusti, M. Albano, M. Marchetti, F. Moglie, M.V. Primiani, Ballistic and electromagnetic shielding behavior of multifunctional Kevlar fiber reinforced epoxy composites modified by carbon nanotubes, Carbon 104 (2016) 141–156, http://dx.doi.org/10.1016/j.carbon.2016.03.059.
[11] R. Pfaendner, Effect of carbon nanotubes on thermal pyrolysis of high density polyethylene and polypropylene, Polym. Degrad. Stab. 95 (2010) 369–373, http://dx.doi.org/10.1016/j.polymdegradstab.2015.06.014.
[12] O. Gutierrez, H. Palza, Effect of carbon nanotubes on thermal pyrolysis of high density polyethylene and polypropylene, Polym. Degrad. Stab. 120 (2015) 122–134, http://dx.doi.org/10.1016/j.polymdegradstab.2015.06.014.
[13] A. Bianco, K. Kostarelos, M. Prato, Making carbon nanotubes biocompatible and biodegradable, Chem. Commun. 47 (2011) 10182–10188, http://dx.doi.org/10.1039/c1cc13011k.
[14] S. Iijima, Helical microtubules of graphitic carbon, Nature (London) 354 (1991) 56–58, http://dx.doi.org/10.1038/354056a0.
[15] J. Aalaie, A. Rahmatpour, S. Maghami, Preparation and characterization of linear low density polyethylene/carbon nanotube nanocomposites, J. Macromol. Sci. Phys. 46 (2007) 877–889, http://dx.doi.org/10.1080/00222340701389100.
[16] W. Tang, M.H. Santare, S.G. Advani, Melt processing and mechanical property characterization of multi-walled carbon nanotube/high density polyethylene (MWNT/HDPE) composite films, Carbon 41 (2003) 2779–2785, http://dx.doi.org/10.1016/S0008-6223(03)00387-7.
[17] H. Ham, Y.S. Choi, I.J. Chung, An explanation of dispersion states of single-walled carbon nanotubes in solvents and aqueous surfactant solutions using solubility parameters, J. Colloid Interface Sci. 286 (2005) 216–223, http://dx.doi.org/10.1016/j.jcis.2005.01.002.

[18] L.S. Cividanes, E.A.N. Simonetti, M.B. Moraes, F.W. Fernandes, G.P. Thim, Influence of carbon nanotubes on epoxy resin cure reaction using different techniques: a comprehensive review, Polym. Eng. Sci. 54 (2013) 1345–1351, http://dx.doi.org/10.1002/pen.23775.
[19] C.Y. Lee, J.H. Bae, T.Y. Kim, S.H. Chang, S.H. Kim, Using silane-functionalized graphene oxides for enhancing the interfacial bonding strength of carbon/epoxy composites, Compos. Part A 75 (2015) 11–17, http://dx.doi.org/10.1016/j.compositesa.2015.04.013.
[20] S. Li, Y. Feng, Y. Li, W. Feng, K. Yoshino, Transparent and flexible films of horizontally aligned carbon nanotube/polyimide composites with highly anisotropic mechanical, thermal, and electrical properties, Carbon 109 (2016) 131–140, http://dx.doi.org/10.1016/j.carbon.2016.07.052.
[21] W.W. Liu, S.P. Chai, A.R. Mohamed, U. Hashim, Synthesis and characterization of graphene and carbon nanotubes: a review on the past and recent developments, J. Ind. Eng. Chem. 20 (2014) 1171–1185, http://dx.doi.org/10.1016/j.jiec.2013.08.028.
[22] M.S. Islam, Y. Deng, L. Tong, S.N. Faisal, A.K. Roy, A.I. Minett, V.G. Comes, Grafting carbon nanotubes directly onto carbon fibers for superior mechanical stability: towards next generation aerospace composites and energy storage applications, Carbon 96 (2016) 701–710, http://dx.doi.org/10.1016/j.carbon.2015.10.002.
[23] F.C. Wang, Z.H. Zhang, Y.J. Sun, Y. Liu, Z.Y. Hu, H. Wang, A.V. Korznikovc, E. Korznikova, Z.F. Liu, S. Osamu, Rapid and low temperature spark plasma sintering synthesis of novel carbon nanotube reinforced titanium matrix composites, Carbon 95 (2015) 396–407, http://dx.doi.org/10.1016/j.carbon.2015.08.061.
[24] J.G. Park, D.H. Keum, Y.H. Lee, Strengthening mechanisms in carbon nanotube-reinforced aluminum composites, Carbon 95 (2015) 690–698, http://dx.doi.org/10.1016/j.carbon.2015.08.112.
[25] R.M. Guedes, C.M.C. Pereira, A. Fonseca, M.S.A. Oliveira, The effect of carbon nanotubes on viscoelastic behaviour of biomedical grade ultra-high molecular weight polyethylene, Compos. Struct. 50 (2013) 263–268, http://dx.doi.org/10.1016/j.compstruct.2013.05.027.
[26] S.L. Ruan, P. Gao, X.G. Yang, T.X. Yu, Toughening high performance ultrahigh molecular weight polyethylene using multiwalled carbon nanotubes, Polymer 44 (2003) 5643–5654, http://dx.doi.org/10.1016/S0032-3861(03)00628-1.
[27] M. Pöllänen, S. Pirinen, M. Suvanto, T.T. Pakkanen, Influence of carbon nanotube-polymeric compatibilizer masterbatches on morphological, thermal, mechanical, and tribological properties of polyethylene, Compos. Sci. Technol. 71 (2011) 1353–1360, http://dx.doi.org/10.1016/j.compscitech.2011.05.009.
[28] S. Maiti, N.K. Shrivastava, S. Suin, B.B. Khatua, polystyrene/MWCNT/graphite nanoplate nanocomposites: efficient electromagnetic interference shielding material through graphite nanoplate-MWCNT-graphite nanoplate networking, ACS Appl. Mater. Interfaces 5 (2013) 4712–4724, http://dx.doi.org/10.1021/am400658h.
[29] X. Wu, X. Chen, J. Wang, J. Liu, Z. Fan, X. Chen, J. Chen, Functionalization of multiwalled carbon nanotubes with thermotropic liquid-crystalline polymer and thermal properties of composites, Ind. Eng. Chem. Res. 50 (2011) 891–897, http://dx.doi.org/10.1021/ie1018029.
[30] A. Kovalchuk, V. Shevchenko, A. Shchegolikhin, P. Nedorezova, A. Klyamkina, A. Aladyshev, Effect of carbon nanotube functionalization on the structural and mechanical properties of polypropylene/mwcnt composites, Macromolecules 41 (2008) 7536–7542, http://dx.doi.org/10.1021/ma801599q.
[31] K. Yang, M. Gu, Y. Guo, X. Pan, G. Mu, Effects of carbon nanotube functionalization on the mechanical and thermal properties of epoxy composites, Carbon 47 (2009) 1723–1737, http://dx.doi.org/10.1016/j.carbon.2009.02.029.
[32] Z. Zhao, Z. Yanga, Y. Hu, J. Li, X. Fan, Multiple functionalization of multi-walled carbon nanotubes with carboxyl and amino groups, Appl. Surf. Sci. 276 (2013) 476–481, http://dx.doi.org/10.1016/j.apsusc.2013.03.119.
[33] L. Cividanes, D. Brunelli, E. Antunes, E. Corat, K. Sakane, G. Thim, Cure study of epoxy resin reinforced with multiwalled carbon nanotubes by raman and luminescence spectroscopy, Appl. Polym. Sci. 27 (2012) 544–553, http://dx.doi.org/10.1002/app.37815.
[34] W. Francisco, F.V. Ferreira, E.V. Ferreira, L.S. Cividanes, A.R. Coutinho, G.P. Thim, Functionalization of multi-walled carbon nanotube and mechanical property of epoxy-Based nanocomposite, J. Aerosp. Technol. Manage. 7 (2015) 289–293, http://dx.doi.org/10.5028/jatm.v7i3.485.
[35] M.J. Sobkowicz, J.R. Dorgan, K.W. Gneshin, A.M. Herring, J.T. McKinnon, Controlled dispersion of carbon nanospheres through surface functionalization, Carbon 47 (2009) 622–628, http://dx.doi.org/10.1016/j.carbon.2008.10.051.
[36] F.V. Ferreira, W. Francisco, B.R.C. Menezes, L.S. Cividanes, A.R. Coutinho, G.P. Thim, Carbon nanotube functionalized with dodecylamine for the effective dispersion in solvents, Appl. Surf. Sci. 357 (2015) 2154–2159, http://dx.doi.org/10.1016/j.apsusc.2015.09.202.
[37] C.L. Morelli, M.N. Belgacem, M.C. Branciforti, R.E.S. Bretas RES, A. Crisci, J. Bras, Supramolecular aromatic interactions to enhance biodegradable film properties through incorporation of functionalized cellulose nanocrystals, Compos. Part A 83 (2016) 80–88, http://dx.doi.org/10.1016/j.compositesa.2015.10.038.
[38] G. Vukovic, A. Marinkovic, M. Obradovic, V. Radmilovic, M. Colic, R. Aleksic, P. Uskokovic, Synthesis, characterization and cytotoxicity of surface amino functionalized water dispersible multiwalled carbon nanotubes, Appl. Surf. Sci. 55 (2009) 8067–8075, http://dx.doi.org/10.1016/j.apsusc.2009.05.016.
[39] X. Ling, Y. Wei, L. Zou, S. Xu, The effect of different order of purification treatments on the purity of multiwalled carbon nanotubes, Appl. Surf. Sci. 276 (2013) 159–166.
[40] S.W. Kim, T. Kim, Y.S. Kim, H.S. Choi, H.J. Lim, S.J. Yang, C.R. Park, Surface modifications for the effective dispersion of carbon nanotubes in solvents and polymers, Carbon 50 (2012) 3–33, http://dx.doi.org/10.1016/j.carbon.2011.08.011.
[41] M. Soares, M. Viana, Z. Schaefer, V. Gangoli, Y. Cheng, V. Caliman, et al., Surface modification of carbon black nanoparticles by dodecylamine: thermal stability and phase transfer in brine medium, Carbon 72 (2014) 287–295, http://dx.doi.org/10.1016/j.carbon.2014.02.008.
[42] A. Rahimpour, M. Jahanshahi, S. Khalili, A. Mollahosseini, A. Zirepour, B. Rajaeian, Novel functionalized carbon nanotubes for improving the surface properties and performance of polyethersulfone (pes) membrane, Desalination 286 (2012) 99–107, http://dx.doi.org/10.1016/j.desal.2011.10.039.
[43] K.N. Kudin, B. Ozbas, H.C. Schniepp, R.K. Prud'homme, I.A. Aksay, R. Car, Raman spectra of graphite oxide and functionalized graphene sheets, Nano Lett. 8 (2008) 36–41, http://dx.doi.org/10.1021/nl071822y.
[44] P.C. Ma, S.Y. Mo, B.Z. Tang, J.K. Kim, Dispersion, interfacial interaction and re-agglomeration of functionalized carbon nanotubes in epoxy composites, Carbon 48 (2010) 1824–1834, http://dx.doi.org/10.1016/j.carbon.2010.01.028.
[45] W. Huang, Y. Wang, G. Luo, F. Wei, 99.9% purity multi-walled carbon nanotubes by vacuum high-temperature annealing, Carbon 41 (2003) 2585–2590.
[46] F.V. Ferreira, W. Francisco, B.R.C. Menezes, F.S. Brito, A.S. Coutinho, L.S. Cividanes, A.R. Coutinho, G.P. Thim, Correlation of surface treatment, dispersion and mechanical properties of HDPE/CNT nanocomposites, Appl. Surf. Sci. 386 (2016) 921–929, http://dx.doi.org/10.1016/j.apsusc.2016.07.164.
[47] X.H. Chen, C.S. Chen, W. Chen, Non-destructive purification of multi-walled carbon nanotubes produced by catalyzed CVD, Mater. Lett. 57 (2002) 734–738, http://dx.doi.org/10.1016/S0167-577X(02)00863-7.
[48] F.L. Jin, C.J. Ma, S.J. Park, Thermal and mechanical interfacial properties of epoxy composites based on functionalized carbon nanotubes, Mater. Sci. Eng A 528 (2011) 8517–8522, http://dx.doi.org/10.1016/j.msea.2011.08.054.
[49] H. Pang, Y. Piao, C. Cui, Y. Bao, J. Lei, G. Yuan, C. Zhang, Preparation and performance of segregated polymer composites with hybrid fillers of octadecylamine functionalized graphene and carbon nanotubes, J. Polym. Res. 20 (2013) 1–8, http://dx.doi.org/10.1007/s10965-013-0304-4.
[50] E.F. Antunes, E.C. Almeida, C.B.F. Rosa, L.I. Medeiros, L.C. Pardini, M. Massi, E.J. Corat, Thermal annealing and electrochemical purification of multi-walled carbon nanotubes produced by camphor/ferrocene mixtures, J. Nanosci. Nanotechnol. 10 (2010) 1296–1303, http://dx.doi.org/10.1166/jnn.2010.1830.
[51] A.H. Barber, S.R. Cohen, S. Kenig, H.D. Wagner, Interfacial fracture energy measurements for multi-walled carbon nanotubes pulled from a polymer matrix, Compos. Sci. Technol. 64 (2004) 2283–2289, http://dx.doi.org/10.1016/j.compscitech.2004.01.023.
[52] M.A.L. Manchado, L. Valentini, J. Biagiotti, J.M. Kenny, Thermal and mechanical properties of single-walled carbon nanotubes-polypropylene composites prepared by melt processing, Carbon 43 (2005) 1499–1505, http://dx.doi.org/10.1016/j.carbon.2005.01.031.
[53] Y. Huang, S. Jiang, L. Wu, Y. Hua, Characterization of LLDPE/nano-SiO2 composites by solid-state dynamic mechanical spectroscopy, Polym. Test. 23 (2004) 9–15, http://dx.doi.org/10.1016/S0142-9418(03)00048-5.
[54] S. Yang, J.T. Tijerina, V.S. Diaz, K. Hernandez, K. Lozano, Dynamic mechanical and thermal analysis of aligned vapor grown carbon nanofiber reinforced polyethylene, Compos. Part B 38 (2007) 228–235, http://dx.doi.org/10.1016/j.compositesb.2006.04.003.
[55] S. Wang, R. Liang, B. Wang, C. Zhang, Reinforcing polymer composites with epoxide-grafted carbon nanotubes, Nanotechnology 19 (2008) 1–7, http://dx.doi.org/10.1088/0957-4484/19/8/085710.
[56] R. Popli, M. Glotin, L. Mandelkern, Dynamic mechanical studies of α and β relaxations of polyethylenes, J. Polym. Sci. 22 (1984) 407–448, http://dx.doi.org/10.1002/pol.1984.180220306.
[57] L. Woo, M.T.K. Ling, A.P. Westphal, Dynamic mechanical analysis (DMA) and low temperature impact properties of metallocene polyethylenes, Thermochim. Acta 272 (1996) 171–179, http://dx.doi.org/10.1016/0040-6031(95)02621-5.
[58] S. Kanagaraj, F.R. Varanda, T.V. Zhiltsova, M.A.S. Oliveira, J.A.O. Simões, Mechanical properties of high density polyethylene/carbon nanotube composites, Compos. Sci. Technol. 67 (2007) 3071–3077, http://dx.doi.org/10.1016/j.compscitech.2007.04.024.
[59] T. McNally, P. Potschke, P. Halley, M. Murphy, D. Martin, S.E.J. Bell, et al., Polyethylene multiwalled carbon nanotube composites, Polymer 46 (2005) 8222–8232, http://dx.doi.org/10.1016/j.polymer.2005.06.094.
[60] E. Assouline, A. Lustiger, A.H. Barber, C.A. Cooper, E. Klein, E. Wachtel, H.D. Wagner, Nucleation ability of multiwall carbon nanotubes in polypropylene composites, J. Polym. Sci. B Polym. Phys. 41 (2003) 520–527, http://dx.doi.org/10.1002/polb.10394.
[61] J. Coleman, U. Khan, W.J. Blau, Y.K. Gun'ko, Small but strong: a review of the mechanical properties of carbon nanotube-polymer composites, Carbon 44 (2006) 1624–1652, http://dx.doi.org/10.1016/j.carbon.2006.02.038.

[62] A.H. Barber, S.R. Cohen, H.D. Wagner, Measurement of carbon nanotube-polymer interfacial strength, Appl. Phys. Lett. 82 (2003) 4140, http://dx.doi.org/10.1063/1.1579568.
[63] J.N. Coleman, M. Cadek, R. Blake, V. Nicolosi, K.P. Ryan, C. Belton, A. Fonseca, J.B. Nagy, Y.K. Gunko, W.J. Blau, High performance nanotube-reinforced plastics: understanding the mechanism of strength increase, Adv. Funct. Mater. 14 (2004) 791–798, http://dx.doi.org/10.1002/adfm.200305200.
[64] X. Shi, B. Jiang, J. Wang, Y. Yang, Influence of wall number and surface functionalization of carbon nanotubes on their antioxidant behavior in high density polyethylene, Carbon 50 (2012) 1005–1013, http://dx.doi.org/10.1016/j.carbon.2011.10.003.
[65] T. Kuila, S. Bose, A.K. Mishra, P. Khanra, N.H. Kim, J.H. Lee, Effect of functionalized graphene on the physical properties of linear low density polyethylene nanocomposites, Polym. Test. 31 (2012) 31–38, http://dx.doi.org/10.1016/j.polymertesting.2011.09.007.
[66] V. Mittal, Gas permeation and mechanical properties of polypropylene nanocomposites with thermally-stable imidazolium modified clay, Eur. Polym. J. 43 (2007) 3727–3736, http://dx.doi.org/10.1016/j.eurpolymj.2007.06.015.
[67] M.A. Osman, V. Mittal, M. Morbidelli, U.W. Suter, Polyurethane adhesive nanocomposites as gas permeation barrier, Macromolecules 36 (2003) 9851–9858, http://dx.doi.org/10.1021/ma035077x.
[68] M.M. Rahman, M. Hosur, A.G. Ludwick, S. Zainuddin, A. Kumar, J. Trovillion, S. Jeelani, Thermo-mechanical behavior of epoxy composites modified with reactive polyol diluent and randomly-oriented amino-functionalized multi-walled carbon nanotubes, Polym. Test. (2012) 777–784, http://dx.doi.org/10.1016/j.polymertesting.2012.05.006.
[69] K. Liao, S. Li, Interfacial characteristics of a carbon nanotube-polystyrene composite system, Appl. Phys. Lett. 79 (9) (2001) 4225, http://dx.doi.org/10.1063/1.1428116.
[70] J.V. Frankland, A. Caglar, D.W. Brenner, J. Griebel, Molecular simulation of the influence of chemical cross-links on the shear strength of carbon nanotube-polymer interfaces, Phys. Chem. B 106 (2002) 3046–3048, http://dx.doi.org/10.1021/jp015591+.
[71] M. Kaseem, K. Hamad, Y.G. Ko, Fabrication and materials properties of polystyrene/carbon nanotube (PS/CNT) composites: a review, Eur. Polym. J. 79 (2016) 36–62, http://dx.doi.org/10.1016/j.eurpolymj.2016.04.011.
[72] S. Nambiar, J.T.W. Yeow, Polymer-composite materials for radiation protection, Appl. Mater. Interfaces 4 (2012) 5717–5726, http://dx.doi.org/10.1021/am300783d.
[73] Y. Yang, M. Gupta, K. Dudley, R. Lawrence, Novel carbon nanotube-polystyrene foam composites for electromagnetic interference shielding, Nano Lett. 5 (2005) 2131–2134, http://dx.doi.org/10.1021/nl051375r.
[74] L. Valentini, I. Armentano, J. Biagiotti, E. Frulloni, J.M. Kenny, S. Santucci, Frequency dependent electrical transport between conjugated polymer and single-walled carbon nanotubes, Diam. Relat. Mater. 12 (2003) 1601–1609, http://dx.doi.org/10.1016/S0925-9635(03)00249-8.
[75] S. Schütte, Effect of chemical functionalization on thermal transport of carbon nanotube composites, Appl. Phys. Lett. 85 (2004) 2229–2231, http://dx.doi.org/10.1063/1.1794370.
[76] W. Lin, Y.H. Xiu, H.J. Jiang, R.W. Zhang, O. Hildreth, K.S. Moon, et al., Self-assembled monolayer-assisted chemical transfer of in-situ functionalized carbon nanotubes, J. Am. Chem. Soc. 90 (2008) 9636–9637, http://dx.doi.org/10.1021/ja802142g.